Measuring the Impact of Outdated Channel State Information in Interference Alignment Techniques

Gerald Artner, Martin Mayer, Maxime Guillaud and Markus Rupp
Institute of Telecommunications, Vienna University of Technology
Gusshausstrasse 25/389, A-1040 Vienna, Austria
Email: gartner@nt.tuwien.ac.at, mmayer@nt.tuwien.ac.at, guillaud@tuwien.ac.at, mrupp@nt.tuwien.ac.at

***Abstract*—Interference alignment has been proposed as a transmission technique to cancel the interference for the K-user interference channel at high signal-to-noise ratio. In the case of multiple-input multiple-output (MIMO)-transmission the interference can be aligned in a subspace of the receiver antennas. In this work we investigate the impact of outdated channel state information (CSI) due to temporal channel variations on the performance of interference alignment. Experimental transmissions of real-time precoded signals from an indoor and outdoor MIMO testbed exhibit performance degradation due to outdated CSI. Furthermore, a model is proposed and evaluated that describes the temporal channel fluctuations based on these measurements.**

I. Introduction

The introduction of interference alignment (IA) has led to a paradigm change in wireless communications. Instead of trying to avoid interference and treating remaining interference as noise, IA attempts to align interference in a subspace separated from the desired signal and cancel the interference at the receiver. IA has been shown to achieve theoretically the maximum degrees of freedom in the K-user interference channel [1].

Simulations with measured channels have shown the feasibility of multiple-input multiple-output (MIMO)-IA [2] and provided a comparison with time division multiple access (TDMA) and interference avoidance [3]. The performance of several IA algorithms was investigated in [4] with measured channels. The first measurement based results have been produced in [5]. In [6] real-time MIMO-IA was compared to TDMA and [7] investigated the impairments of channel state information (CSI) errors in the same setup. A measurement based comparison to coordinated multipoint can be found in [8]. In our previous work [9], we presented measurements of IA with real-time CSI feedback and transmission of precoded signals. Measurements performed with the same setup in [10] suggest that IA might be limited by transmitter noise for high signal-to-noise ratio (SNR).

In this paper we present a measurement based evaluation and modeling of IA impairments due to outdated channels. We propose a practical approach to estimate the mutual information and an autoregressive model that reflects the temporal orthogonal frequency-division multiplexing (OFDM) MIMO channel variations.

The remainder of this paper is organized as follows. In Section II we provide a short overview of IA techniques. The testbed for the measurement and the measurement scenario are explained in Section III and the measurement method is described in Section IV. In Section V we propose several approaches to model our observations. Those models are compared to the measured results in Section VI. In Section VII we summarize the findings of this paper.

II. Interference Alignment in the K-User MIMO Interference Channel

We assume a MIMO interference channel model comprising K transmitters with N_T antennas each and K receivers with N_R antennas each, where transmitter j is considered the desired transmitter for receiver i if and only if $i = j$ and is considered an interferer if $i \neq j$. Furthermore, if we assume a $N_\mathrm{T} \times d$ linear filter $\mathbf{V}_j$ at each transmitter j, and additive white Gaussian noise $\mathbf{n}_i$, then the signal at receiver i reads

$$\mathbf{y}_i = \sum_{j=1}^{K} \mathbf{H}_{ij}\mathbf{V}_j\mathbf{s}_j + \mathbf{n}_i, \tag{1}$$

where $\mathbf{H}_{ij}$ denotes the $N_\mathrm{R} \times N_\mathrm{T}$ channel matrix from transmitter j to receiver i and $\mathbf{s}_j$ is the signal from transmitter j with unit variance. A linear zero-forcing $d \times N_\mathrm{R}$ filter $\mathbf{U}_i^H$ is then applied at each receiver

$$\mathbf{r}_i = \underbrace{\mathbf{U}_i^H\mathbf{H}_{ii}\mathbf{V}_i\mathbf{s}_i}_{\text{desired signal}} + \underbrace{\sum_{j\neq i}^{K} \mathbf{U}_i^H\mathbf{H}_{ij}\mathbf{V}_j\mathbf{s}_j}_{\text{interference}} + \underbrace{\mathbf{U}_i^H\mathbf{n}_i}_{\text{effective noise}}. \tag{2}$$

The goal of IA is to align and cancel the interference at receiver i such that

$$\mathbf{U}_i^H\mathbf{H}_{ij}\mathbf{V}_j = \mathbf{0}, \forall i \neq j, \tag{3}$$

while retaining full rank at each desired link

$$\mathrm{rank}(\mathbf{U}_i^H\mathbf{H}_{ii}\mathbf{V}_i) = d. \tag{4}$$

A necessary feasibility condition for IA was presented in [11]:

$$N_T + N_R - (K+1)d \geq 0. \tag{5}$$

III. Measurement Setup

The Vienna MIMO testbed (VMTB) is a system for wireless communications that operates at a commercial 2.503 GHz frequency. It contains two outdoor ($j = 1, 2$) and one indoor[1] ($j = 3$) transmitter as well as one moveable indoor receiver. The outdoor transmitters are located on rooftops of adjacent buildings. They are set up at roughly 150 m distance to the receiver. The outdoor transmitters are equipped with four cross polarised antennas from Kathrein (800 10543). The indoor transmitter employs two Kathrein 800 10677 with two cross polarised antennas each. The four $\lambda/2$-dipole antennas of the receiver are located inside a laptop chassis. The chassis is mounted to a positioning table that allows movement of the receive antennas in the horizontal plane and an azimuthal orientation between 0° and 120°. The receiver is depicted in Figure 1.

No streets lie between transmitters and receiver but there are several trees. No people or large moving parts were present in the laboratory during measurements. All measurements were performed on sunny days with wind speed less than 5 km/h.

As $\mathbf{U}_i$ and $\mathbf{V}_j$ are calculated from channel estimates, $\widehat{\mathbf{H}}_{ij}$ have to be collected from the receivers and distributed to all nodes. The receiver and the transmitters are connected with a fiber network. The CSI is distributed over the fiber network for all experiments

[1] When comparing with [9], note that the indoor transmitter was moved to the same room as the receiver.

978-1-4799-1481-4/14/$31.00 ©2014 IEEE

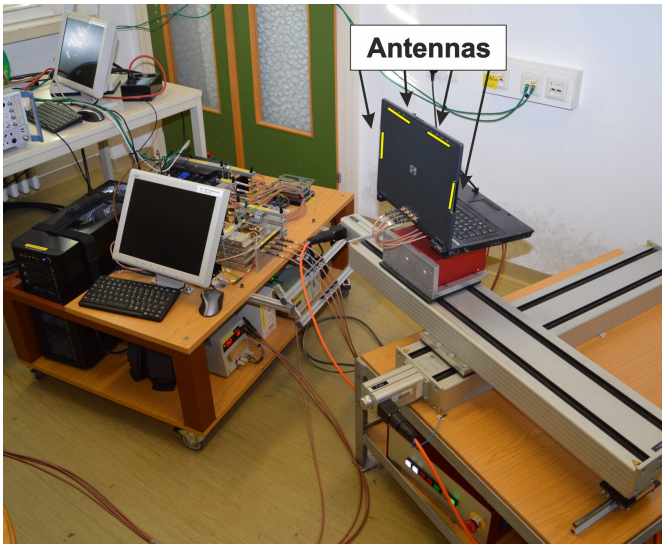

Fig. 1. Receiver of the VMTB: the radio frequency equipment and monitoring computer are shown on the left. On the right are the four dipole antennas inside a laptop chassis that is mounted to a positioning table.

conducted as part of this work. Additionally this network supports the synchronization of the timing units and allows to send messages between the computer programs.

Data symbols are transmitted by OFDM, but to keep calculation times low, only one subcarrier is active. The estimated OFDM channel matrices $\widehat{\mathbf{H}}_{ij}$ are obtained with a least squares approach. Each block of data symbols is prefixed with a pilot sequence. The time intervals between consecutive transmissions are not equally long, a transmission is started as soon as all computations are finished and the transmitters have synchronized. The average time between consecutive transmissions is 49.2 ms. Because only one receiver is available on the VMTB, channel matrices for two virtual receivers are generated iid from a complex Gaussian distribution. These channels are known to all nodes without estimation errors and are kept constant for all transmissions.

IV. Measurement Methodology

The performance of IA depends on accurate channel estimates to calculate the precoding and receive filters and on the assumption that these channels remain constant during the transmission of the signals. An experiment was performed in order to evaluate the performance of IA with outdated CSI and quantify its impairments.

The laptop chassis with the receive antennas moves to a random position on the positioning table and a random azimuthal orientation. At this position p, the signals are transmitted in a frame l precoded with $\mathbf{V}_j^{(l,p)}$ and the receiver applies $\mathbf{U}_i^{(l,p)H}$ to suppress the interference. In a typical operation mode these filters need to be updated regularly. To measure the effects of outdated CSI, the filters obtained from the channel of the first frame are however kept constant for all $N_l = 210$ frames at position p:

$$\mathbf{V}_j^{(p)} = \mathbf{V}_j^{(1,p)} \text{ and } \mathbf{U}_i^{(p)} = \mathbf{U}_i^{(1,p)} \tag{6}$$

It is expected that the channel varies over time, which leads to reduced performance due to outdated $\mathbf{V}_j^{(p)}$ and $\mathbf{U}_j^{(p)H}$.

Afterwards the receive antennas are moved to another position and the filters of the first frame are again kept. To mitigate the impact of small scale fading, this measurement is performed at $N_p = 50$ positions and measurement results are averaged over this ensemble.

V. Proposed Channel Model

We propose the following measure to approximate the mutual information (MI):

$$\begin{aligned} R_i^{(l,p)} =& \log_2 \det \Bigg(\mathbf{I} + \mathbf{U}_i^{(p)H} \widehat{\mathbf{H}}_{ii}^{(l,p)} \mathbf{V}_i^{(p)} \left(\mathbf{U}_i^{(p)H} \widehat{\mathbf{H}}_{ii}^{(l,p)} \mathbf{V}_i^{(p)} \right)^H \\ & \left(\sum_{j \neq i}^{K} \mathbf{U}_i^{(p)H} \widehat{\mathbf{H}}_{ij}^{(l,p)} \mathbf{V}_j^{(p)} \left(\mathbf{U}_i^{(p)H} \widehat{\mathbf{H}}_{ij}^{(l,p)} \mathbf{V}_j^{(p)} \right)^H + \right. \\ & \left. \mathbf{U}_i^{(p)H} \widehat{\mathbf{Q}}_{N,i}^{(l,p)} \mathbf{U}_i^{(p)} \right)^{-1} \Bigg), \end{aligned} \tag{7}$$

where $R_i^{(l,p)}$ is the proposed measure at receiver i, frame l and position p, $\widehat{\mathbf{H}}_{ij}^{(l,p)}$ are channel matrices of the different models and $\mathbf{Q}_{N,i}^{(l,p)}$ is the $N_\mathrm{R} \times N_\mathrm{R}$ covariance matrix of the additive noise at receiver i.

This is different from the approach in [9, Equation 10], where the mutual information was estimated as

$$\widehat{\mathrm{MI}} = \log_2 \det \left(\widehat{\mathbf{Q}}_a \widehat{\mathbf{Q}}_b^{-1} \right), \tag{8}$$

where $\widehat{\mathbf{Q}}_a$ is the covariance matrix estimate obtained from a part of the received signal that contains the desired signal, interference and noise. Covariance matrix $\widehat{\mathbf{Q}}_b$ is estimated from another part of the received signal that contains only interference and noise.

We propose an autoregressive model to reflect the channel variations. We have investigated a variety of such models with different complexity:

- **Measurement**
  Channel matrices $\widehat{\mathbf{H}}_{ij}^{(l,p)}$ are estimated from a measured pilot sequence that was transmitted over the air interface. The noise covariance matrices $\widehat{\mathbf{Q}}_{N,i}^{(l,p)}$ are estimated from a noise gap in the transmit signal. The noise gap is a part of the transmit signal where $\mathbf{s}_j = \mathbf{0} \; \forall \; j$.
- **Measurement with simplified noise**
  The estimated channel matrices $\widehat{\mathbf{H}}_{ij}^{(l,p)}$ from the measurements are kept, but the $\widehat{\mathbf{Q}}_{N,i}^{(l,p)}$ term is replaced with a simpler description. We model the additive noise as Gaussian with covariance $\sigma_N^2 \mathbf{I}$, with unit matrix $\mathbf{I}$ of size $N_R \times N_R$, that is, independent of the individual receive antenna with

  $$\sigma_N^2 = \frac{1}{N_l N_p N_R} \sum_{l=1}^{N_l} \sum_{p=1}^{N_p} \mathrm{trace} \left(\widehat{\mathbf{Q}}_{N,i}^{(l,p)} \right). \tag{9}$$

  We can omit the receiver index i because the VMTB has only one physical receiver. This simplified noise is applied in all further models.
- **AR**(n)
  The temporal channel variations are modeled as autoregressive (AR) processes of order n:

  $$f^{(l)} = v^{(l)} + a_1 f^{(l-1)} + a_2 f^{(l-2)} + \ldots + a_n f^{(l-n)}. \tag{10}$$

  In a first step signal rotations due to frequency offset of the estimated channel matrices over time are compensated for:

  $$\mathbf{H}_{ij}^{\prime(l,p)} = \mathrm{e}^{j\widehat{\theta}_{ij}^{(p)}} \widehat{\mathbf{H}}_{ij}^{(l,p)}, \tag{11}$$

  with $\widehat{\theta}_{ij}^{(p)}$ chosen such that any rotation with respect to $\mathbf{H}_{ij}^{(1,p)}$ is reversed. This does not affect IA performance.
  Then the line-of-sight (LOS)-mean is subtracted

  $$\overline{\mathbf{H}}_{ij}^{(p)} = \frac{1}{N_l} \sum_{l=1}^{N_l} \mathbf{H}_{ij}^{\prime(l,p)}. \tag{12}$$

The coefficients a_n of the AR-model of order n are then calculated by solving the Yule-Walker equation for all elements in the $N_R \times N_T$ matrices $\mathbf{H}_{ij}^{\prime(l,p)} - \overline{\mathbf{H}}_{ij}^{(p)}$ and for all p, i and j. The sequences f are finally collected in $\mathbf{F}_{ij}^{(l,p)}$.
Before evaluating Equation (7) the LOS-mean is again added:

$$\mathbf{H}_{ij}^{(l,p)} = \mathbf{F}_{ij}^{(l,p)} + \overline{\mathbf{H}}_{ij}^{(p)}. \tag{13}$$

- **AR(n) with random mean**
  This model is the same as 'AR(n)' except that all elements of $\overline{\mathbf{H}}_{ij}^{(p)}$ are iid complex random variables drawn from a zero mean Gaussian distribution. The LOS-means $\overline{\mathbf{H}}_{ij}^{(p)}$ from transmitter j are generated with variance

$$\sigma_{H,j}^2 = \frac{1}{N_l N_p} \sum_{l=1}^{N_l} \sum_{p=1}^{N_p} \mathrm{var}\left(\widehat{\mathbf{H}}_{ij}^{(l,p)}\right). \tag{14}$$

  Again because only one receiver is available on the VMTB, we omit the receiver index i.

VI. Verification and Results

Figure 2 shows the results obtained from measured channels. The curves are averaged over $N_p = 50$ receiver positions and are shown with 95% confidence intervals. The transmissions are temporally 49.2 ms apart on average.

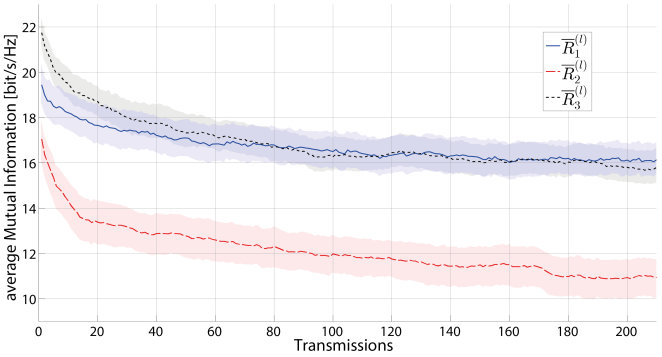

Fig. 2. Performance Measure $\overline{R}_i^{(l)}$ with $\widehat{\mathbf{H}}_{ij}^{(l,p)}$ estimated from measurements for all three transmitters over time (1 transmission ≈ 49.2 ms), mean and 95% confidence intervals averaged over $N_p = 50$ positions.

The performance without receive-filters $\mathbf{U}_i^{(p)H}$ is also of interest. In this case the performance measure is evaluated as

$$R_i^{\prime(l,p)} = \log_2 \det\left(\mathbf{I} + \widehat{\mathbf{H}}_{ii}^{(l,p)} \mathbf{V}_i^{(p)} \left(\widehat{\mathbf{H}}_{ii}^{(l,p)} \mathbf{V}_i^{(p)}\right)^H \left(\sum_{j \neq i}^{K} \widehat{\mathbf{H}}_{ij}^{(l,p)} \mathbf{V}_j^{(p)} \left(\widehat{\mathbf{H}}_{ij}^{(l,p)} \mathbf{V}_j^{(p)}\right)^H + \widehat{\mathbf{Q}}_{N,i}^{(l,p)}\right)^{-1}\right). \tag{15}$$

$R_i^{\prime(l,p)}$ for $i = 1, 2, 3$ are depicted in Figures 3–5, along with the estimated MI between the transmit signal before the transmit filters $\mathbf{V}_j^{(p)}$ and the received signal without $\mathbf{U}_i^{(p)H}$ applied. The theoretically achievable rate of IA, that is when the interference can be cancelled entirely, is

$$R_{i,\mathrm{noInt}}^{\prime(l,p)} = \log_2 \det\left(\mathbf{I} + \widehat{\mathbf{H}}_{ii}^{(l,p)} \mathbf{V}_i^{(p)} \left(\widehat{\mathbf{H}}_{ii}^{(l,p)} \mathbf{V}_i^{(p)}\right)^H \widehat{\mathbf{Q}}_{N,i}^{(l,p)\,-1}\right). \tag{16}$$

The lower bound, at which it is not reasonable to apply IA is calculated as

$$R_{i,\mathrm{TMDA/noCSI}}^{\prime(l,p)} = \log_2 \det\left(\mathbf{I} + \widehat{\mathbf{H}}_{ii}^{(l,p)} \widehat{\mathbf{H}}_{ii}^{(l,p)\,H} \widehat{\mathbf{Q}}_{N,i}^{(l,p)\,-1}\right). \tag{17}$$

This rate $R_{i,\mathrm{TMDA/noCSI}}^{\prime(l,p)}$ is divided by K to obtain the conjectured rate for interference avoidance approaches such as TDMA.

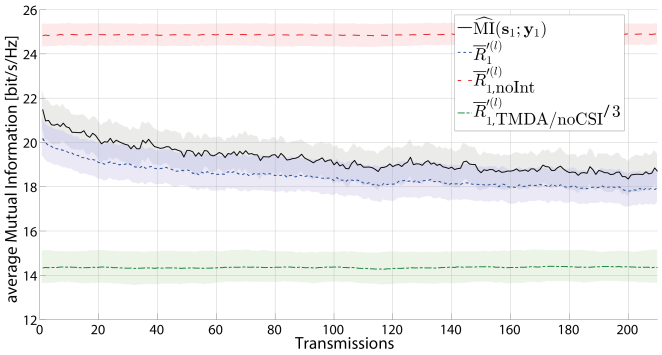

Fig. 3. Performance Measure $\overline{R}_1^{\prime(l)}$ with $\widehat{\mathbf{H}}_{1j}^{(l,p)}$ estimated from measurements for desired transmitter one over time (1 transmission ≈ 49.2 ms), mean and 95% confidence intervals averaged over $N_p = 50$ positions.

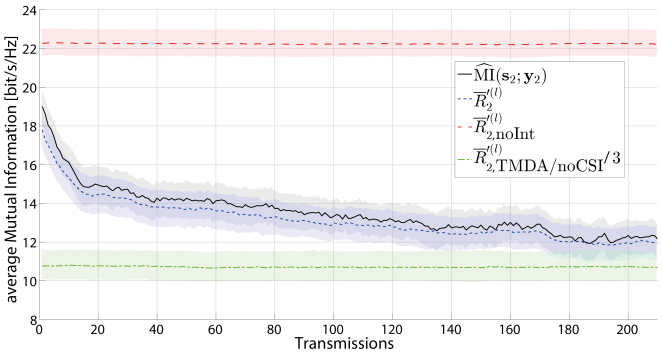

Fig. 4. Performance Measure $\overline{R}_2^{\prime(l)}$ with $\widehat{\mathbf{H}}_{2j}^{(l,p)}$ estimated from measurements for desired transmitter two over time (1 transmission ≈ 49.2 ms), mean and 95% confidence intervals averaged over $N_p = 50$ positions.

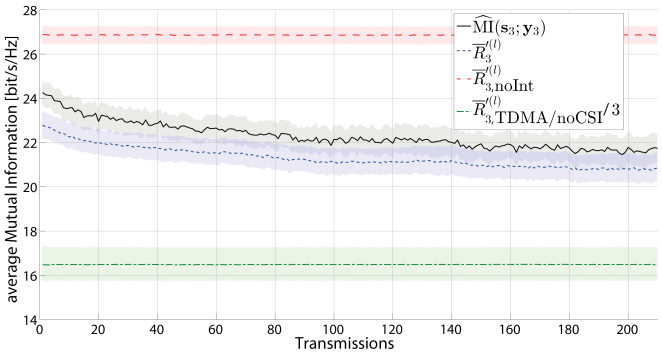

Fig. 5. Performance Measure $\overline{R}_3^{\prime(l)}$ with $\widehat{\mathbf{H}}_{3j}^{(l,p)}$ estimated from measurements for desired transmitter three over time (1 transmission ≈ 49.2 ms), mean and 95% confidence intervals averaged over $N_p = 50$ positions.

Figure 6 compares the models from Section V. As example the measurement and models for transmitter $j = 3$ are shown. The 'Measurement with simplified noise' leads to a relatively small deviation from 'Measurement', which justifies the use of the simplified noise model in all subsequent models.

The outcome of the stochastic models varies. $\overline{R}_i^{(l)}$ for measurements are averaged over $N_p = 50$, those from simulations are averaged over $N = 20N_p = 1000$. Figure 7 shows the influence of the order n of the AR model. $\overline{R}_i^{(l)}$ of 'AR(n)' flatten too fast,

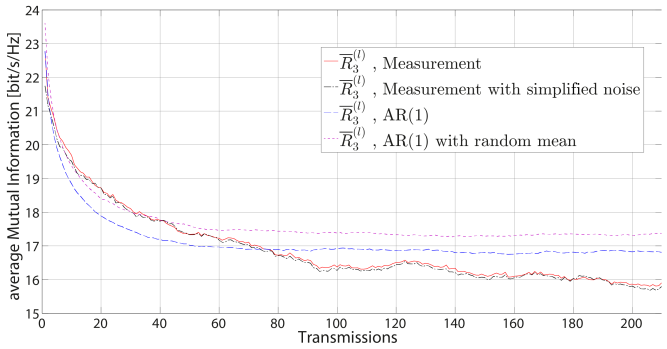

Fig. 6. Comparison of different models on the example of $\overline{R}_3^{(l)}$. Measurements are averaged over $N_p = 50$ positions, simulations of AR(n) are averaged over $N = 20N_p$.

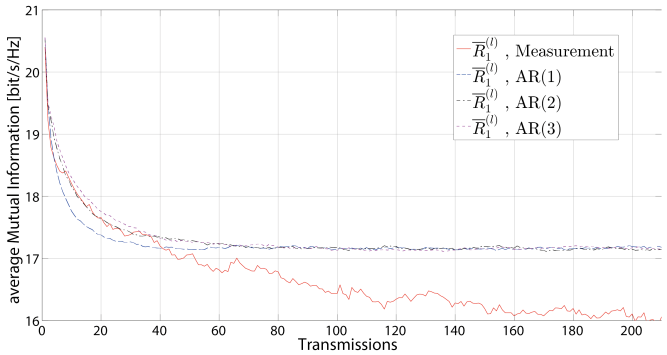

Fig. 7. Influence of the order of the AR model shown on the example of $\overline{R}_1^{(l)}$. Measurements are averaged over $N_p = 50$ positions, simulations of AR(n) are averaged over $N = 20N_p$. Because AR(3), AR(10) and AR(20) overlap visually, only AR(3) is depicted.

leaving room for improved models. The mean squared error (MSE) between the simulated and the measured curves is then calculated between these ensemble averages and listed in Table I.

Description	MSE
AR(1)	0.54
AR(2)	0.53
AR(3)	0.53
AR(10)	0.54
AR(1) with random mean	1.20

TABLE I
COMPARISON OF THE MSE BETWEEN $\overline{R}_1^{(l)}$ WITH MEASURED $\widehat{\mathbf{H}}_{1j}^{(l,p)}$ AND SEVERAL MODELS

Table II lists evaluated parameters for several models. The SNR at the receiver i is calculated as

$$\mathrm{SNR}_i = 10\log_{10}\left(P_{\mathrm{RX}ii}/\sigma_{\mathrm{N}}^2\right), \tag{18}$$

$$P_{\mathrm{RX}ij} = \frac{1}{N_l N_p N_R}\sum_{l=1}^{N_l}\sum_{p=1}^{N_p}\mathrm{trace}\left[\mathrm{vec}\left(\widehat{\mathbf{H}}_{ij}^{(l,p)}\right)\mathrm{vec}\left(\widehat{\mathbf{H}}_{ij}^{(l,p)}\right)^H\right]. \tag{19}$$

The power of the transmit signal is normalized to unity. The signal-to-interference ratio (SIR) is defined as

$$\mathrm{SIR}_i = 10\log_{10}\left(\frac{P_{\mathrm{RX}ii}}{\sum_{j\neq i}P_{\mathrm{RX}ij}}\right). \tag{20}$$

Model	Parameter
Measurement	$\mathrm{SNR}_{i=[1\,2\,3]} = [39.40\ \ 39.73\ \ 39.07]\ dB$
	$\mathrm{SIR}_{i=[1\,2\,3]} = [-3.28\ -3.30\ -4.01]\ dB$
M. with simplified noise	$\sigma_N^2 = 0.1381$
AR(n) with random mean	$\sigma_{H,j=[1\,2\,3]}^2 = [310.8\ \ 175.8\ \ 593.2]$

TABLE II
EVALUATED FIGURES FOR THE MEASUREMENT AND MODELS

VII. CONCLUSION

In this paper we have investigated the performance impairments of interference alignment due to outdated filters in a quasi-static scenario. We have quantified these effects with measurements and proposed autoregressive (AR) models of varying complexity that describe these measurements.

ACKNOWLEDGMENT

This work has been funded by the Christian Doppler Laboratory for Wireless Technologies for Sustainable Mobility, KATHREIN-Werke KG, and A1 Telekom Austria AG. This work was also supported by the FP7 project HIATUS (grant #265578) of the European Comission and by the Austrian Science Fund (FWF) under project grants S10606 and S10611 within the National Research Network SISE. The financial support by the Federal Ministry of Economy, Family and Youth and the National Foundation for Research, Technology and Development is gratefully acknowledged.

REFERENCES

[1] V. Cadambe and S. Jafar, "Interference alignment and degrees of freedom of the K-user interference channel," *IEEE Transactions on Information Theory*, vol. 54, pp. 3425–3441, Aug 2008.

[2] O. El Ayach, S. Peters, and R. Heath, "Real world feasibility of interference alignment using MIMO-OFDM channel measurements," in *Military Communications Conference*, 2009.

[3] O. El Ayach, S. Peters, and R. Heath, "The feasibility of interference alignment over measured MIMO-OFDM channels," *IEEE Transactions on Vehicular Technology*, vol. 59, no. 9, pp. 4309–4321, 2010.

[4] R. Brandt, H. Asplund, and M. Bengtsson, "Interference alignment in frequency - a measurement based performance analysis," in *19th International Conference on Systems, Signals and Image Processing (IWSSIP 2012)*, pp. 227–230, 2012.

[5] S. Gollakota, S. D. Perli, and D. Katabi, "Interference alignment and cancellation," in *ACM SIGCOMM Computer Communication Review*, vol. 39, pp. 159–170, ACM, 2009.

[6] O. González, D. Ramirez, I. Santamaria, J. Garcia-Naya, and L. Castedo, "Experimental validation of interference alignment techniques using a multiuser MIMO testbed," in *2011 International ITG Workshop on Smart Antennas (WSA)*, IEEE, 2011.

[7] J. Garcıa-Naya, L. Castedo, O. González, D. Ramırez, and I. Santamaria, "Experimental evaluation of interference alignment under imperfect channel state information," *Proc. EUSIPCO 2011, Barcelona*, 2011.

[8] P. Zetterberg and N. Moghadam, "An experimental investigation of SIMO, MIMO, interference-alignment (IA) and coordinated multi-point (CoMP)," in *19th International Conference on Systems, Signals and Image Processing (IWSSIP 2012)*, pp. 211–216, 2012.

[9] M. Mayer, G. Artner, G. Hannak, M. Lerch, and M. Guillaud, "Measurement based evaluation of interference alignment on the Vienna MIMO testbed," in *Proceedings of the Tenth International Symposium on Wireless Communication Systems (ISWCS 2013), Ilmenau*, 2013.

[10] M. Mayer, M. Guillaud, G. Artner, and M. Rupp, "Measurement and modelling of interference alignment impairments," in *8th IEEE Sensor Array and Multichannel Signal Processing Workshop (SAM)*, 2014.

[11] C. Yetis, T. Gou, S. Jafar, and A. Kayran, "On feasibility of interference alignment in MIMO interference networks," *IEEE Transactions on Signal Processing*, vol. 58, pp. 4771–4782, Sept 2010.